Journal of Thermal Analysis and Calorimetry, Vol. 85 (2006) 2, 321–327

THERMAL AND X-RAY DIFFRACTION STUDIES OF THE SOLID–SOLID INTERACTIONS IN CuO–MoO$_3$/MgO SYSTEM

H. G. El-Shobaky[*]

Chemistry Department, Faculty of Science, Cairo University, Egypt

The solid–solid interactions in pure and MoO$_3$-doped CuO/MgO system were investigated using TG, DTA and XRD. The composition of pure mixed solids were 0.1CuO/MgO, 0.2CuO/MgO and 0.3CuO/MgO and the concentrations of MoO$_3$ were 2.5 and 5 mol%. These solids were prepared by wet impregnation of finely powdered basic magnesium carbonate with solutions containing calculated amounts of copper nitrate and ammonium molybdate followed by heating at 400–1000 °C.

The results revealed that ammonium molybdate doping of the system investigated enhanced the thermal decomposition of copper nitrate and magnesium hydroxide which decomposed at temperatures lower than those observed in case of the undoped mixed solids by 70 and 100°C, respectively. A portion of CuO present dissolved in the lattice of MgO forming CuO–MgO solid solution with subsequent limited increase in its lattice parameter. The other portion interacted readily with a portion of MoO$_3$ at temperatures starting from 400°C yielding CuMoO$_4$ which remained stable up to 1000°C. The other portion of MoO$_3$ interacted with MgO producing MgMoO$_4$ at temperatures starting from 400°C and remained also stable at 1000°C. The diffraction peaks of Cu$_2$MgO$_3$ phase were detected in the diffractograms of pure and MoO$_3$-doped 0.3CuO/MgO precalcined at 1000°C. The formation of this phase was accompanied by an endothermic peak at 930°C.

Keywords: *Cu$_2$MgO$_3$, CuMoO$_4$, CuO, MgMoO$_4$, MgO, MoO$_3$, solid solution*

Introduction

Thermally decomposed metal nitrates and metal carbonates have been used as precursors in chemical industries, as catalysts, in metallurgical processes and as electrochemical power sources [1–12]. The structures formed when metals are deposited on the surfaces of metal oxides can be quite complex. The initial monolayers may involve in the formation of different oxides, leading effectively to oxide/oxide interfaces. These interfaces are of great importance in a variety of technological areas, including heterogeneous catalysis [13–17].

Pure ammonium molybdate decomposed into MoO$_3$ at 340°C [18]. Supporting of ammonium molybdate on different support surfaces changes its decomposition temperature in the sequence: MgO<unsupported<ZrO$_2$, Al$_2$O$_3$<SiO$_2$<Nb$_2$O$_5$ [19]. It was found that ammonium molybdate decomposed at 280°C in Co$_3$O$_4$–MoO$_3$/MgO system [20].

MoO$_3$-treatment of Al$_2$O$_3$–TiO$_2$ [21], La$_2$O$_3$–TiO$_2$, In$_2$O$_3$–TiO$_2$ [22] and Co$_3$O$_4$/Al$_2$O$_3$ [23] systems prepared by impregnation had been characterized by XRD, XPS, FTIR and O$_2$ chemisorption techniques. The characterization studies revealed that the MoO$_3$ concentration on the surface is greater than in the bulk of the solids due to the high dispersion of MoO$_3$ on the support surface. Mixing of MoO$_3$ with another oxides may lead to the formation of solid solutions as in the case of (*i*) V$_2$O$_5$–MoO$_3$ system a solid solution of a composition $(V_2O_5)_{1-x}$–$(MoO_3)_x$ with $0\leq x\leq 1$ is formed at 423 K [24]. (*ii*) Solid solutions in a formula Cr$_{1-x}$Al$_x$VMoO$_7$, where x=0.65 are formed in the system CrVMoO$_7$–AlVMoO$_7$ [25]. (*iii*) Also a solid solution was formed in the system V$_2$O$_5$–MoO$_3$–Sb$_2$O$_4$ [26]. The Mo(VI) ions are incorporated into the crystal lattice of SbVO$_5$ instead of both Sb(V) and V(V) and the limit of solubility of MoO$_3$ in SbVO$_5$ does not exceed 20 mol%.

On the other hand, MoO$_3$ may interact with the other mixed oxides with production of molybdate compounds. In case of NiO–MoO$_3$ [18], Co$_3$O$_4$–MoO$_3$/MgO [20], MoO$_3$/TiO$_2$–ZrO$_2$ [27], Co$_3$O$_4$–MoO$_3$/Al$_2$O$_3$ [28], Nb$_2$O$_5$–MoO$_3$ [29] and MoO$_3$–A$_2$CO$_3$ or A$_2$MoO$_4$ (*A*=Na, K, Rb, Cs) [30] systems the corresponding molybdates were separated CoMoO$_4$, NiMoO$_4$, ZrMo$_2$O$_8$ and CoMoO$_4$, Nb$_{14}$Mo$_3$O$_{44}$, Nb$_{12}$MoO$_{33}$, A$_2$Mo$_4$O$_{13}$ ·xH$_2$O (x=2–6), respectively.

The systems NiO–MgO, MnO–MgO, ZnO–MgO and Al$_2$O$_3$–MgO forming solid solutions were investigated by different techniques [31–36]. In the Al$_2$O$_3$–MgO system the range of solid solution was from 0 to 20 mass% Al$_2$O$_3$. The lattice parameter of MgO phase decreased with increasing the amount of alumina due to the increased amount of Al$_2$O$_3$ dissolved in the MgO lattice with subsequent formation of the solid solution. Calcination of (48 mass%)

---

[*] hala_elshobaky@yahoo.com

1388–6150/$20.00

© 2006 Akadémiai Kiadó, Budapest

Akadémiai Kiadó, Budapest, Hungary
Springer, Dordrecht, The Netherlands

CoO/MgO at 500 and 800°C led to the formation of CoO–MgO solid solution. While the calcination of (4–48 mass%) CoO/MgO at 900°C led to formation of Co_2MgO_4 compound [35].

The present investigation reports a study of solid-solid interactions in the $CuO–MoO_3/MgO$ system. The techniques employed were DTA, TG and XRD. These techniques allowed us to clarify the effects of MoO_3 treatment on the thermal behaviour of mixed solids prepared by the wet impregnation method and to identify the different phases produced by heating the mixed solids at various temperatures.

Experimental

Materials

Pure CuO/MgO samples were prepared by treating a known mass of finely powdered basic magnesium carbonate, $MgCO_3{\cdot}Mg(OH)_2$, with different amounts of copper nitrate dissolved in the least amount of distilled water making pastes. The proportions of copper nitrate were calculated so that the molar compositions of the calcined solids were 0.1CuO/MgO, 0.2CuO/MgO and 0.3CuO/MgO. The pastes thus obtained were dried at 120°C and then calcined for 5 h in air at 400, 600, 800 and 1000°C. The $CuO–MoO_3/MgO$ mixed solids were prepared by treating a known mass of basic magnesium carbonate with copper nitrate solution containing different proportions of it, drying at 120°C and then treating the dried solids with ammonium molybdate solution. The resulting materials were then dried at 120°C and calcined for 5 h in air at 400, 600, 800 and 1000°C. The concentrations of ammonium molybdate solution employed corresponded to the addition of 2.5 and 5 mol% MoO_3 (with respect to the sum of MgO and CuO).

The nominal molar compositions of the calcined mixed solids were 0.1CuO/MgO (I), 0.2CuO/MgO (II) and 0.3CuO/MgO (III). The prepared mixed solid specimens were designated CuMg–I, CuMg–I–2.5Mo, CuMg–I–5Mo, CuMg–II, CuMg–II–2.5Mo, CuMg–II–5Mo, CuMg–III, CuMg–III–2.5Mo and CuMg–III–5Mo. All chemicals employed were of analytical grade and supplied BDH company.

Methods

TG and DTA of various uncalcined materials were carried out using Shimadzu DTA-50H systems. The rate of heating was kept at 10°C min^{-1}. The analyses were followed at temperatures between room temperature and 1000°C with α-Al_2O_3 as a reference material. A 40 mg sample of each solid specimen was employed in each case. The measurements were carried out in a current of nitrogen flowing at a rate of 50 cm^3 min^{-1}.

An X-ray investigation of the thermal products of the different mixed solids was performed with a Philips diffractometer (type PW 1390). The patterns were run with nickel filtered copper radiation (λ=1.5405 Å) at 36 kV and 16 mA with scanning speed 2° in 2θ min^{-1}.

Results and discussion

The thermal behaviour of pure and doped mixed solids

TG of CuMg–I, CuMg–I–5Mo, CuMg–III and CuMg–III–5Mo performed. Figure 1 depicts the TG curves of CuMg–I, CuMg–I–5Mo, CuMg–III and CuMg–III–5Mo. The obtained curves vary between three and six steps. The different values of mass loss processes calculated in each process for various solids permitted to deduce the chemical change corresponding each step.

The results obtained are given in Table 1. Inspection of Table 1 reveals the following: (*i*) The TG curves of CuMg–I mixed solids consist of three steps. The first step extends between 80 and 130°C, the second between 254.6 and 369.4°C and the last between 376.6 and 406.4°C. These steps correspond to the removal of physisorbed water, decomposition of copper nitrate and basic magnesium carbonate, respectively. The last two steps can be represented by the following equations:

$$0.1Cu(NO_3)_2 + \\ +0.5MgCO_3{\cdot}Mg(OH)_2 \xrightarrow{\text{mass loss (11.4\%), 254.6–369.4°C}} \\ 0.1CuO+0.5MgCO_3{\cdot}Mg(OH)_2+0.2NO_2+0.1O_2$$

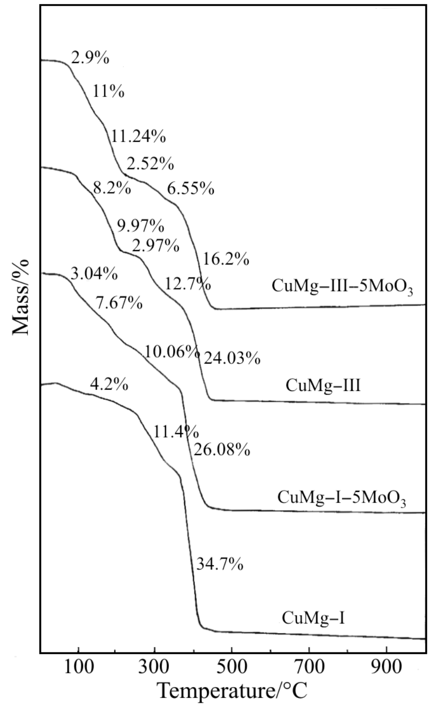

Fig. 1 TG curves of uncalcined pure and MoO_3-doped mixed solids

Table 1 TG data of pure and treated uncalcined mixed solids

Solid	T/°C	Mass loss/%		Decomposition steps
		found	calculated	
0.1CuO/MgO (CuMg–I)	80–130	4.2	–	physisorbed water
	254.6–369.4	11.4	11.6	decomposition of copper nitrate
	376.6–406.4	34.7	34.7	decomposition of basic magnesium carbonate
0.1CuO/MgO +5 mol% MoO$_3$ (CuMg–I–5Mo)	80–140	I) 3.04	–	physisorbed water
	180–220	II) 7.67	11.5 for copper nitrate+amm. molybdate	steps II+III are corresponding to decomposition of copper nitrate+amm. molybdate+2/3 of magnesium hydroxide
	261–374	III) 10.06	9.2 for total magnesium hydroxide	
	374.5–450	IV) 26.08	22.6 magnesium carbonate	step IV is corresponding to the decomposition of the last 1/3 magnesium hydroxide+total decomposition of magnesium carbonate
0.3CuO/MgO (CuMg–III)	130–170	I) 8.2	–	physisorbed water
	177–208	II) 9.97	25.4 copper nitrate (the sum of steps II+III+IV=25.64)	decomposition of copper nitrate
	208–273	III) 2.97		
	312–381	IV) 12.7		
	397–436	V) 24.03	24.3	decomposition of basic magnesium carbonate
0.3CuO/MgO +5mol% MoO$_3$ (CuMg–III–5Mo)	90–110	I) 2.9	–	physisorbed water
	110–170	II) 11	24.6 copper nitrate+amm. molybdate (the sum of steps II+III+IV=24.76)	steps II+III+IV are corresponding to decomposition of copper nitrate+amm. molybdate
	170–210	III) 11.2		
	210–300	IV) 2.52		
	300–385	V) 6.55	6.6	decomposition of magnesium hydroxide
	403–430	VI) 16.2	16.2	decomposition of magnesium carbonate

$$0.1CuO+0.5MgCO_3\cdot Mg(OH)_2\xrightarrow{\text{mass loss (34.7\%), 376.6–406.4°C}}0.1CuO+MgO+0.5CO_2+0.5H_2O$$

(*ii*) CuMg–I–5–Mo mixed solids decompose via four steps. The thermal change accompanying each step is given in the last column in Table 1. These changes can be represented by the following reactions:

$$\begin{gathered}0.1Cu(NO_3)_2+0.05/7(NH_4)_6Mo_7O_{24}+\\+0.5MgCO_3\cdot Mg(OH)_2\xrightarrow{\text{mass loss (14.4\%), 180–374°C}}\\0.1CuO+0.05MoO_3+0.17MgCO_3\cdot Mg(OH)_2+\\+0.33MgO+0.333MgCO_3+0.2NO_2+0.043NH_3+\\0.355H_2O+0.23O_2\end{gathered}$$

$$\begin{gathered}0.1CuO+0.05MoO_3+0.17MgCO_3\cdot Mg(OH)_2+\\0.33MgO+0.33MgCO_3\xrightarrow{\text{mass loss (26.08\%), 374.5–450°C}}\\0.1CuO+0.05MoO_3+0.5MgO+0.25O_2+\\+0.5CO_2+0.17H_2O\end{gathered}$$

The produced evolved NO$_2$, O$_2$, CO$_2$ and NH$_3$ have not been detected and their formation was speculatively suggested in the light of TG measurements. (*iii*) CuMg–III and CuMg–III–5Mo were decomposed via five and six steps, respectively. The first step corresponds to removal of physisorbed water. The second, third and fourth steps correspond to the decomposition of copper nitrate besides ammonium molybdate in CuMg–III–5Mo sample in temperature ranges between 177–381 and 110–300°C in CuMg–III and CuMg–III–5Mo, respectively. The final decomposition step in CuMg–III takes place at a temperature range between 397–436°C is the decomposition of basic magnesium carbonate to magnesium oxide. In case of CuMg–III–5Mo magnesium hydroxide was decomposed firstly in a temperature range 300–395°C then magnesium carbonate decomposed to magnesium oxide at a temperature range of 403–430°C. From these results it can be concluded that ammonium molybdate doping of copper nitrate and basic magnesium carbonate mixed solids enhanced the thermal decomposition of both copper nitrate and magnesium hydroxide which decomposed at temperatures lower than those in case of the undoped mixed solids by 70 and 100°C, respectively.

DTA curves of CuMg–II, CuMg–II–5Mo, CuMg–III and CuMg–III–5Mo were determined and illustrated in Fig. 2. The DTA curves of CuMg–II, CuMg–II–5Mo, CuMg–III exhibit six endothermic peaks while DTA curves of CuMg–III–5Mo consist of seven endothermic peaks. The minima of these peaks are found at 90–100, 191–205, 295, 338, 378–392, 410–434 and 930°C. Most of these peaks are strong and sharp. The first set of peaks indicates the departure of physisorbed water. The set of peaks located at 191–205 and 295°C correspond to the thermal decomposition of copper nitrate and ammonium molybdate in case of the doped samples. The peak located at 338°C is found only in CuMg–III–5Mo sample which is indicative for the decomposition of magnesium hydroxide. The peaks located at 378–392°C and 410–434°C characterize the thermal decomposition of basic magnesium carbonate in case of CuMg–II, CuMg–II–5Mo, CuMg–III and indicative for the decomposition of magnesium carbonate in case of CuMg–III–5Mo. The final endothermic peaks located at 930°C correspond to the formation of a new CuO–MgO compound. The identification of the newly formed compound will be examined by XRD investigation of the solids preheated at 1000°C.

XRD investigation of various solids

X-ray diffractograms of various mixed solids preheated at 400, 600, 800 and 1000°C were measured. These results are summarized in Table 2 which shows the effect of calcination temperature, CuO content and dopant concentration on the peak height of some selected peaks located at certain *d*-spacings relative to individual oxides and produced compounds. Table 2 reveals that the diffractograms of various mixed solid samples and those treated with MoO_3 precalcined in air at 400°C consist of diffraction peaks of well crystalline MgO phase and CuO phase with moderate degree of crystallinity. The mixed solid samples treated with 5 mol% MoO_3 consist of magnesium molybdate $MgMoO_4$ as a minor phase besides the MgO and CuO phases. The formation of $MgMoO_4$ is accompanied by a progressive decrease in the peak height of the diffraction peaks characteristic to MgO phase. It can also be seen that doping of the investigated system with 5 mol% MoO_3 decreases the peak height of all diffraction peaks of CuO phase. This observed decrease in the peak height of the CuO peaks may be attributed to possible solid-solid interaction between CuO and MoO_3 with production of an amorphous $CuMoO_4$ phase.

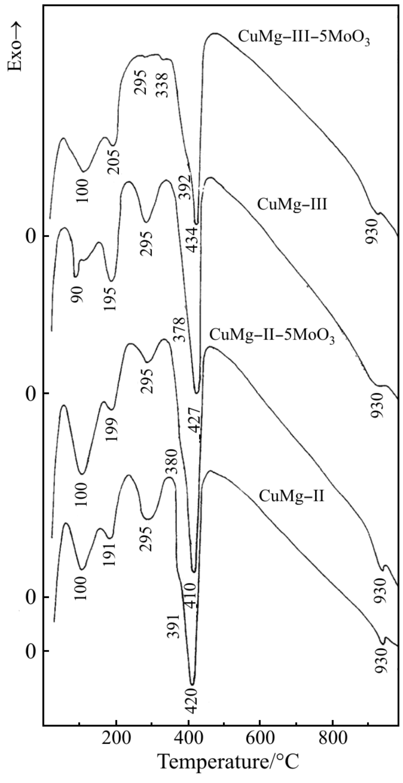

Fig. 2 DTA curves of uncalcined pure and MoO_3-doped mixed solids

Preliminary experiments showed that the thermal decomposition of ammonium molybdate in air at 400°C resulted in the formation of well crystalline orthorhombic MoO_3. The fact that the amounts of MoO_3 added (4 and 8 mass% MoO_3) is below the detection limit of X-ray diffractometer might suggest that most of molybdenum species added was concentrated in the uppermost surface layers of the mixed solids. In other words, the concentration of MoO_3 on the top surface layers should be much greater than the nominal amount added. This behaviour is expected because doped solids were prepared by the wet impregnation method and not by coprecipitation [37]. The absence of all diffraction peaks of MoO_3 in the patterns of the mixed oxides indicates its complete conversion into $MgMoO_4$ and $CuMoO_4$ phases.

The X-ray diffractograms of different pure mixed solids investigated precalcined at 400°C revealed also that the increase in the concentration of CuO from 0.1 to 0.3 mol/mol MgO is accompanied by an increase in the degree of crystallinity CuO phase and a decrease in the peak height of MgO phase. So, the increased concentration of CuO inhibits the crystallization of MgO.

Table 2 shows that for pure and doped mixed oxide solids, raising the calcination temperature to 600°C is accompanied by an increase in the peak heights of MgO, CuO and $MgMoO_4$ phases besides the appearance of the diffraction peaks of $CuMoO_4$ phase upon doping with 5 mol% MoO_3. For the pure and MoO_3 treated CuMg–II solids the intensities of the diffraction peaks relative to $MgMoO_4$ increase as a function of MoO_3 added. The increase in the abundance of $MgMoO_4$ and the formation of $CuMoO_4$

Table 2 The effect of precalcination temperature and composition on the height of some diffraction lines h (a. u.*)

Solid	$T_{calcination}$/ °C	d=1.216 Å 26% MgO	d=1.87 Å 32% CuO	d=3.29 Å 68% CuMoO$_4$	d=1.93 Å 21% MgMoO$_4$	d=3.35 Å 67% CuMoO$_4$+ 100% MgMoO$_4$	d=2.28 Å 100% Cu$_2$MgO$_3$
0.1CuO/MgO	400	70	5	–	–	–	–
+2.5 mol% MoO$_3$		65	–	–	–	–	–
+5 mol% MoO$_3$		47	–	–	–	1.5	–
0.2CuO/MgO		65	18	–	–	–	–
+2.5 mol% MoO$_3$		59	11	–	–	–	–
+5 mol% MoO$_3$		32	8	–	2.5	6	–
0.3CuO/MgO		48	40	–	–	–	–
+2.5 mol% MoO$_3$		37	30	–	–	–	–
+5 mol% MoO$_3$		28	18	–	4	15	–
0.1CuO/MgO	600	100	15	–	–	–	–
+2.5 mol% MoO$_3$		90	12	–	5	22	–
+5 mol% MoO$_3$		80	9	7	6	32	–
0.2CuO/MgO		85	28	–	–	–	–
+2.5 mol% MoO$_3$		78	23	–	9	35	–
+5 mol% MoO$_3$		62	17	12	11	62	–
0.3CuO/MgO		65	42	–	–	–	–
+2.5 mol% MoO$_3$		59	36	–	11	43	–
+5 mol% MoO$_3$		40	29	18	14	84	–
0.1CuO/MgO	800	148	32	–	–	–	–
+2.5 mol% MoO$_3$		132	21	11	15	108	–
+5 mol% MoO$_3$		118	18	29	31	210	–
0.2CuO/MgO		135	75	–	–	–	–
+2.5 mol% MoO$_3$		120	69	25	14	104	–
+5 mol% MoO$_3$		110	58	52	32	233	–
0.3CuO/MgO		102	102	–	–	–	–
+2.5 mol% MoO$_3$		87	90	16	11	87	–
+5 mol% MoO$_3$		66	75	31	17	138	–
0.1CuO/MgO	1000	194	–	–	–	–	–
+2.5 mol% MoO$_3$		176	–	14	13	89	–
+5 mol% MoO$_3$		169	–	35	29	185	–
0.2CuO/MgO		163	–	–	–	–	–
+2.5 mol% MoO$_3$		144	–	23	10	88	–
+5 mol% MoO$_3$		139	–	35	20	147	–
0.3CuO/MgO		145	–	–	–	–	63
+2.5 mol% MoO$_3$		120	–	8	8	53	50
+5 mol% MoO$_3$		115	–	17	17	100	35

*a. u. arbitrary unit; *d* is the *d* spacing

phases are evidenced by the progressive decrease in the peak height of the diffraction peaks of MgO and CuO phases.

The diffractograms of pure mixed solid oxides CuMg–I, CuMg–II and CuMg–III solids and those treated with 2.5 and 5 mol% MoO$_3$ and then precalcined at 800°C (Table 2) consisted of MgO and CuO phases, are similar to all investigated mixed solids preheated at 600°C. Moreover, the diffraction peaks of MgMoO$_4$ and CuMoO$_4$ appeared in case of other solid samples treated with 2.5 and 5 mol% MoO$_3$ and preheated at 800°C. It is clear that the increase in both the calcination temperature and the amount of MoO$_3$ added enhanced much the solid–solid interactions between MoO$_3$ and both MgO and CuO producing MgMoO$_4$ and CuMoO$_4$. On the other hand, the peak heights of MgO, MgMoO$_4$ and CuMoO$_4$ suffer a measurable decrease (Table 2) due to increasing the concentration of CuO from 16.67 to 23.08 mol% (0.2CuO/MgO, 0.3CuO/MgO). In the case of CuMg–II–5Mo, the peak height at 1.216 Å (MgO phase 26%), 3.289 Å (CuMoO$_4$ phase 68%) and at 1.93 Å (MgMoO$_4$ phase 21%) were found to decrease from 110 to 66 (a. u.), 52 to 31 (a. u.) and 32 to 17 (a. u.), respectively (Table 2). This finding may be discussed in terms of a possible dissolution of CuO in MgO matrix forming a solid solution. This speculation is confirmed by the observed limited increase in the lattice parameter (Table 3) of MgO (ionic radius of Mg^{2+}=0.66 Å) upon increasing the concentration of CuO (ionic radius of Cu^{2+}=0.72 Å). The lattice parameter of MgO in pure mixed oxide solids precalcined at 800°C increased from 4.2058 to 4.2145 Å. Also the lattice parameter of MgO in heavily doped mixed oxide solids calcined at 800°C increased from 4.2020 to 4.2116 Å (Table 3). The observed limited increase in the lattice parameter of MgO phase may be attributed to the small difference in the ionic size of Mg^{2+} and Cu^{2+}. The decrease in the peak heights of MgO, $MgMoO_4$ and $CuMoO_4$ due to increasing the concentration of CuO from 0.2 to 0.3 mol/mol MgO may indicate that CuO much preferably dissolves in MgO lattice rather than interacting with MoO_3 producing a solid solution.

Table 2 shows that the diffractograms of the pure and doped CuMg–I, CuMg–II and CuMg–III solids precalcined at 1000°C consist, only, of the diffraction peaks of MgO phase and new diffraction peaks characteristic to Cu_2MgO_3 phase in case of pure and doped CuMg–III (rich in CuO only) besides the $MgMoO_4$ and $CuMoO_4$ phases. In fact, the observed endothermic peak located at 930°C in the case of the system rich in copper stands as evidence for the formation of Cu_2MgO_3 phase. The absence of any diffraction peaks of this compound in the case of pure and MoO_3–doped CuMg–II precalcined at 1000°C although the appearance of endothermic peak at 930°C suggests that its amount is below the detection limit of the X-ray diffractometer.

The complete disappearance of all diffraction peaks of CuO as a separate phase in all solids precalcined at 1000°C clearly indicates its complete dissolution in MgO lattice forming CuO–MgO solid solution as detected from Table 3 which shows that the lattice parameter of MgO decreased progressively by increasing the amount of CuO. The diffraction lines of this new compound are separated only at the highest concentration of CuO. Table 2 reveals that raising the calcination temperature to 1000°C is accompanied by: (*i*) An increase in peak height of MgO indicating an effective improvement in its degree of crystallinity. (*ii*) A decrease in the intensities of the diffraction peaks of $CuMoO_4$ phase as a result of an enhanced formation of Cu_2MgO_3. (*iii*) The peak heights of $MgMoO_4$ were not changed on raising the calcination temperature from 800 to 1000°C. This finding suggests that the solid–solid interactions between MoO_3 and MgO reach their maximum limit at 800°C i.e raising the calcination temperature to 1000°C did not affect the enhancement of the $MgMoO_4$ formation. (*iv*) The intensity of the Cu_2MgO_3 peaks decreased on doping with MoO_3 due to the CuO–MoO_3 interactions. In other words, MoO_3-doping of the system investigated opposes the formation of Cu_2MgO_3 compound.

Inspection of Table 3 shows clearly that the progressive increase of MgO lattice due to dissolution of some of copper ions is maximum at 400°C and minimum at 1000°C in case of the pure solid samples. This finding might indicate that heat treatment of MgO treated with CuO species at 400°C led mainly to the formation of CuO–MgO solid solution. The increase in calcination temperature above this limit led to an enhanced formation of CuO–MgO compound. In fact at 1000°C the sample rich in CuO gave some diffraction peaks of Cu_2MgO_3 phase, indicating that most of CuO underwent solid–solid interaction with MgO at such high temperature.

Table 3 Lattice parameter of pure and heavily MoO_3-doped CuO/MgO mixed solids

Solid	$T_{calcination}$/°C	Lattice parameter/Å
0.1CuO/MgO	400	4.1980
0.2CuO/MgO		4.2029
0.3CuO/MgO		4.2092
0.1CuO/MgO	600	4.2019
0.2CuO/MgO		4.2070
0.3CuO/MgO		4.2119
0.1CuO/MgO	800	4.2058
0.2CuO/MgO		4.2130
0.3CuO/MgO		4.2145
0.1CuO/MgO	1000	4.2074
0.2CuO/MgO		4.2150
0.3CuO/MgO		4.2190
0.1CuO–5MoO_3/MgO	400	4.1975
0.2CuO–5MoO_3/MgO		4.2002
0.3CuO–5MoO_3/MgO		4.2025
0.1CuO–5MoO_3/MgO	600	4.1985
0.2CuO–5MoO_3/MgO		4.2035
0.3CuO–5MoO_3/MgO		4.2085
0.1CuO–5MoO_3/MgO	800	4.2020
0.2CuO–5MoO_3/MgO		4.2057
0.3CuO–5MoO_3/MgO		4.2116
0.1CuO–5MoO_3/MgO	1000	4.2064
0.2CuO–5MoO_3/MgO		4.2100
0.3CuO–5MoO_3/MgO		4.2155

Conclusions

- Ammonium molybdate doping of the investigated mixed solids much stimulates the thermal decomposition of copper nitrate and dehydroxylation of basic magnesium carbonate by 70 and 100°C, respectively.
- MoO_3 interacted readily with magnesium oxide and copper oxide at temperatures starting from 400°C to produce $MgMoO_4$ and $CuMoO_4$,which remained thermally stable up to 1000°C.
- A portion of copper oxide reacts with MoO_3 to yield $CuMoO_4$ while the other portion dissolved completely in the matrix of MgO producing CuO–MgO solid solution.
- Copper oxide interacted readily with MgO at 930°C yielding a new compound of formula Cu_2MgO_3 compound.

References

1 T. Matsuda, H. Taguchi and M. Nagao, J. Thermal Anal., 38 (1992) 1835.
2 T. J. Taylor, D. Dollimore and G. A. Gamlen, Thermochim. Acta, 103 (1986) 333.
3 A. H. Carim, P. Doherty, T. T. Kodas and K. Ott, Mater. Lett., 8 (1989) 335.
4 L. Gubrynowicz, Thermochim. Acta, 239 (1994) 181.
5 A. Kaddouri, C. Mazzocchia, E. Tempesti, R. Nomen and J. Sempere, J. Thermal Anal., 53 (1998) 533.
6 R. Sokoll, H. Hobert and I. Schmuck, J. Catal., 121 (1990) 153.
7 F.-L. Wang and T.-F. Tsai, Appl. Catal. A, 201 (2000) 91.
8 S. Poulston, N. J. Price, C. Weeks, M. D. Allen, P. Parlett, M. Steinberg and M. Bowker, J. Catal., 178 (1998) 658.
9 I. Balint and K.-I. Aika, Appl. Catal. A, 196 (2000) 209.
10 Y. Lu, J. Xue, C. Yu, Y. Liu and S. Shen, Appl. Catal. A, 174 (1998) 121.
11 S. Lanfredi, S. Folgueras-Dominguez and A. C. M. Rodrigues, J. Mater. Chem., 5 (1995) 1957.
12 L. E. B. Malta, V. R. Caffarena, M. E. Medeiros and T. Ogasawara, J. Therm. Anal. Cal., 75 (2004) 901.
13 H. H. Kung, Transition Metal Oxides: Surface Chemistry and Catalysis, Elsevier, Amsterdam 1989.
14 J. C. Volt, in Adsorption and Catalysis on Oxide Surface, Ed. M. Che and G. C. Bond, Elsevier, Amsterdam 1985, pp. 331–342.
15 E. Ruckenstein and H. Y. Wang, Appl. Catal. A, 198 (2000) 33.
16 J. Ziolkowski, A. M. Maltha, H. Kist, E. J. Grootendorst, H. J. M. de Groot and V. Ponec, J. Catal., 160 (1996) 148.
17 S. Meijers, T. P. Pruys van der Hoeven, V. Ponec, J. P. Jacobs and H. H. Brongersma, J. Catal., 161 (1996) 459.
18 W. M. Shaheen, Mater. Lett., 52 (2002) 272.
19 C. Thomazeau, V. Martin and P. Afanasiev, Appl. Catal. A, 199 (2000) 61.
20 N. R. E. Radwan, A. M. Ghozza and G. A. El-Shobaky, Thermochim. Acta, 398 (2003) 211.
21 B. M. Reddy, B. Chowdhurya, E. P. Reddy and A. Fernandez, Appl. Catal. A, 213 (2001) 279.
22 B. M. Reddy, B. Chowdhury and P. G. Smirniotis, Appl. Catal. A, 219 (2001) 53.
23 G. A. El-Shobaky, A. M. Ghozza, A. A. El Warraky and G. M. Mohamed, Colloids Surf. A, 219 (2003) 97.
24 K. V. Madhuri, B. S. Naidu, O. M. Hussain, M. Eddrief and C. Julien, Mater. Sci. Eng. B, 86 (2001) 165.
25 P. Tabero and E. Filipek, J. Therm. Anal. Cal., 77 (2004) 183.
26 E. Filipek, J. Therm. Anal. Cal., 74 (2003) 477.
27 B. M. Reddy, B. Chowdhury, E. P. Reddy and A. Fernández, J. Mol. Catal. A, 162 (2000) 431.
28 G. A. El-Shobaky, A. G. Ghozza and G. M. Mohamed, Appl. Catal. A, 241 (2003) 235.
29 P. Tabero, J. Therm. Anal. Cal., 74 (2003) 491.
30 N. L. Misra, K. D. S. Mudher and V. Venugopal, J. Therm. Anal. Cal., 76 (2004) 737.
31 Z. Kluz, J. Stoch and T. Czeppe, Z. Phys. Chem. (Munich), 134 (1983) 125.
32 A. V. Kuznetsov, I. K. Vorontsova and I. D. Mikheikin, Russ. J. Phys. Chem. (Engl. Transl.), 71 (1997) 1081.
33 V. Jayaram and B. S. Rani, Mater. Sci. A, 304 (2001) 800.
34 L. Shuzhi, Z. Bangwei, S. Xiaolin, O. Yifang, X. Haowen and X. Zhongyu, J. Mater. Process. Technol., 89 (1999) 405.
35 H. Y. Wang and E. Ruckenstein, Appl. Catal. A, 209 (2001) 207.
36 A. M. Salem, M. Mokhtar and G. A. El-Shobaky, Solid State Ionics, 170 (2004) 33.
37 G. A. El-Shobaky, A. N. Al-Noaimi and T. M. H. Saber, Bull. Soc. Chim. Fr., 6 (1987) 930.

Received: November 18, 2004
Accepted: January 3, 2005

DOI: 10.1007/s10973-004-6842-6